AD-A080 080 SRI INTERNATIONAL MENLO PARK CA F/G 16/4
CALCULATION OF THE RESPONSE OF ADAPTION KITS IN ACCIDENTAL SIDE--ETC(U)
NOV 79 J K GRAN, L E SCHWER DAAK10-78-C-0158
UNCLASSIFIED NL

| OF |
ADA
080080

END
DATE FILMED
2-80
DDC

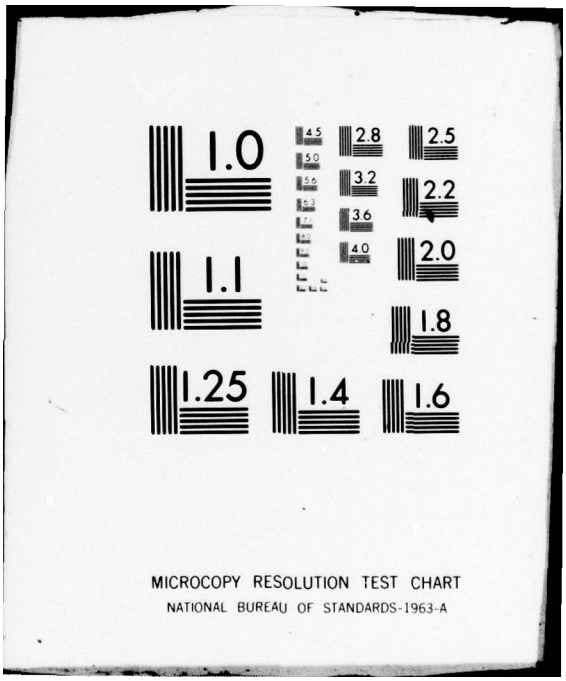
1.0
1.1
1.25
1.4
1.6
1.8
2.0
2.2
2.5
2.8
3.2
3.6
4.0
4.5
5.0
5.6
6.3
MICROCOPY RESOLUTION TEST CHART
NATIONAL BUREAU OF STANDARDS-1963-A

LEVEL II

(1)

SC

(11) November 1979

(9) Bimonthly Progress Report No. 8, 3 Jul - 2 Sep 79,
Covering the Period 3 July through 2 September 1979

(6) CALCULATION OF THE RESPONSE OF ADAPTION KITS IN ACCIDENTAL SIDE IMPACTS.

By: (10) J. K. Gran and L. E. Schwer

(12) 24

Prepared for:

DEPARTMENT OF THE ARMY
Attention: W. Bowman
U.S. Army Armament R&D Command
Dover, New Jersey 07801

Attention: SARPA-ND-C

(15) Contract No. DAAK10-78-C-0158 (new)
SRI International Project PYU-7422

Approved:

J. D. Colton

J. D. Colton, Project Supervisor
Engineering Mechanics Department

G. R. Abrahamson, Laboratory Director
Poulter Laboratory

SRI International
333 Ravenswood Ave. • Menlo Park, California 94025
(415) 326-6200 • Cable: SRI INTL MPK • TWX: 910-373-1246

JOB

410 281

INTRODUCTION

This report describes the current study of the response of adaption kits in accidental side impacts. The primary goal of the project is the further development of finite element models for a generic missile structure so that adaption kit response, particularly component accelerations, can be predicted for side impacts of the missile. An additional goal is experimental determination of the impact response of a missile structure that contains a hard link safe-arm device.

The work planned for this contract consists of four tasks. In Task 1, we are further developing finite element models for substructures and checking the models' predictions against experimental data. In Task 2, we are using the models to calculate the response of complete structures, again by comparing the predictions with experimental results insofar as feasible. In Task 3, we are transferring the analytical capabilities developed in Tasks 1 and 2 by implementing the SUPER code at ARRADCOM. In Task 4, we are performing impact experiments on scale models of a specific prototype missile structure to help plan some full-scale tests. For a more detailed description of Tasks 1 through 3, refer to Bimonthly Progress Report No. 1, July 1978. Task 4 is described fully in Bimonthly Progress Report No. 3, November 1978.

During this reporting period, progress was made in Tasks 1 and 2. The estimated percentage of the work completed is shown in Figure 1. The remainder of the report describes the technical progress and future plans for each task and indicates the financial status of the contract.

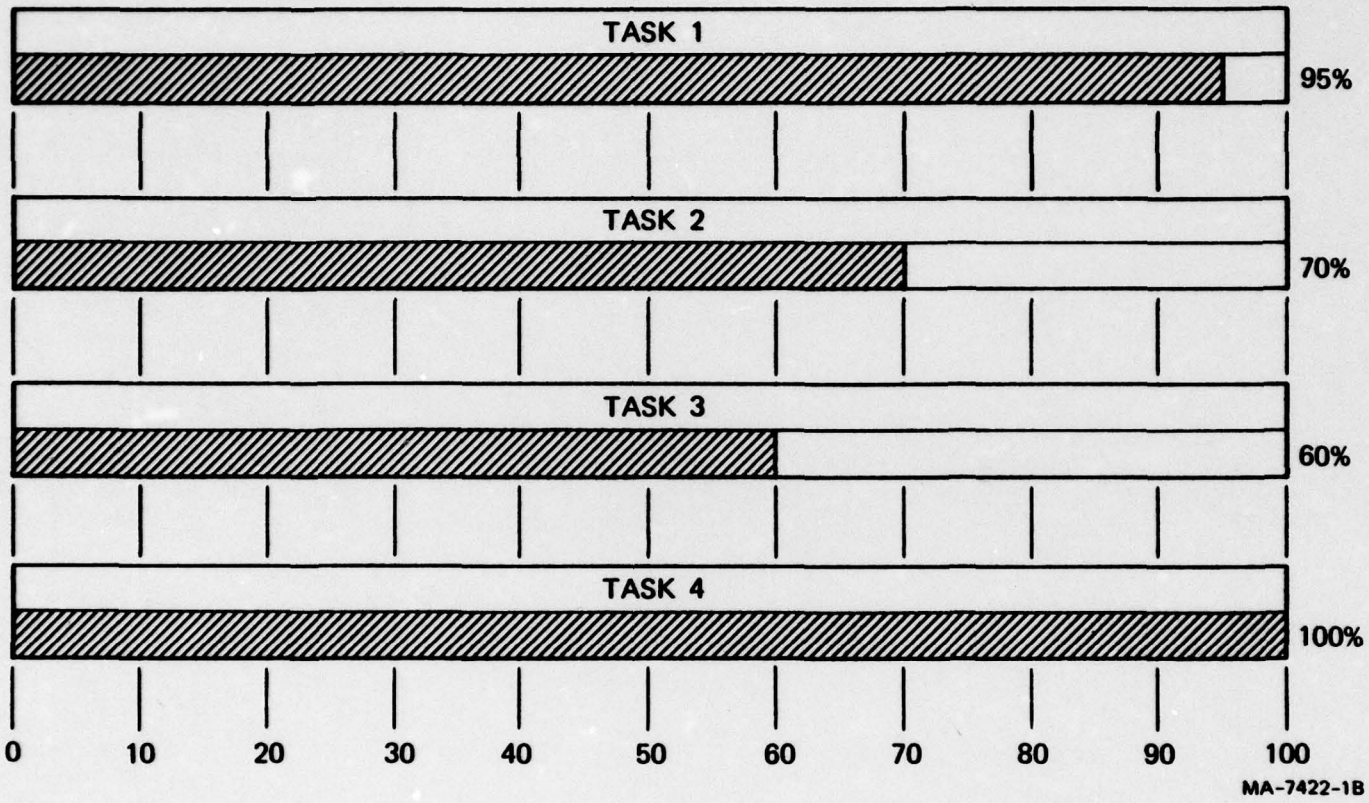

FIGURE 1 ESTIMATED PERCENT WORK COMPLETED BY TASK
2 SEPTEMBER 1979

II PROGRESS

Task 1: Development of Finite Element Models for Substructures

The exploratory experiments described previously[1] demonstrated that in the generic structure being studied, we must be able to analyze the response of the ring independently from the response of the plate. This report describes the analysis of the response of the ring alone using impact experiments and the SUPER code.

The ring response was studied with a series of experiments and calculations in which the complexity of the problem was gradually increased. First, the elastic response of a flat ring was studied to develop a basic analytic model for rings with impact loads. Second, the elastic response of an L-section ring was studied to check the model with the more complex geometry. Third, the elastic-plastic response of an L-section ring was studied to assess the ring model with plasticity. Fourth, an L-section ring in a shell was studied in order to include shell effects in the model.

Elastic Response of a Flat Ring

The first experiment in the ring study was a low-speed impact of a flat ring without a shell. This experiment was conducted so that a simple ring geometry could be studied. The rectangular cross section of the ring measured 6.4 mm by 12.7 mm; the outside diameter was 99.8 mm. The ring geometry is shown in Figure 2(a). The ring material was 6061-T6 aluminum. Strain gages with an element length of 6.4 mm were mounted at several locations on the inside rim of the ring to measure circumferential strains. The gage locations are also shown in Figure 2(a). The ring was launched so that it struck the steel barrier edge-on in free flight at a speed of 6.9 m/s. At this impact velocity, the response of the ring is entirely elastic except for the very localized plastic flow at the impact point.

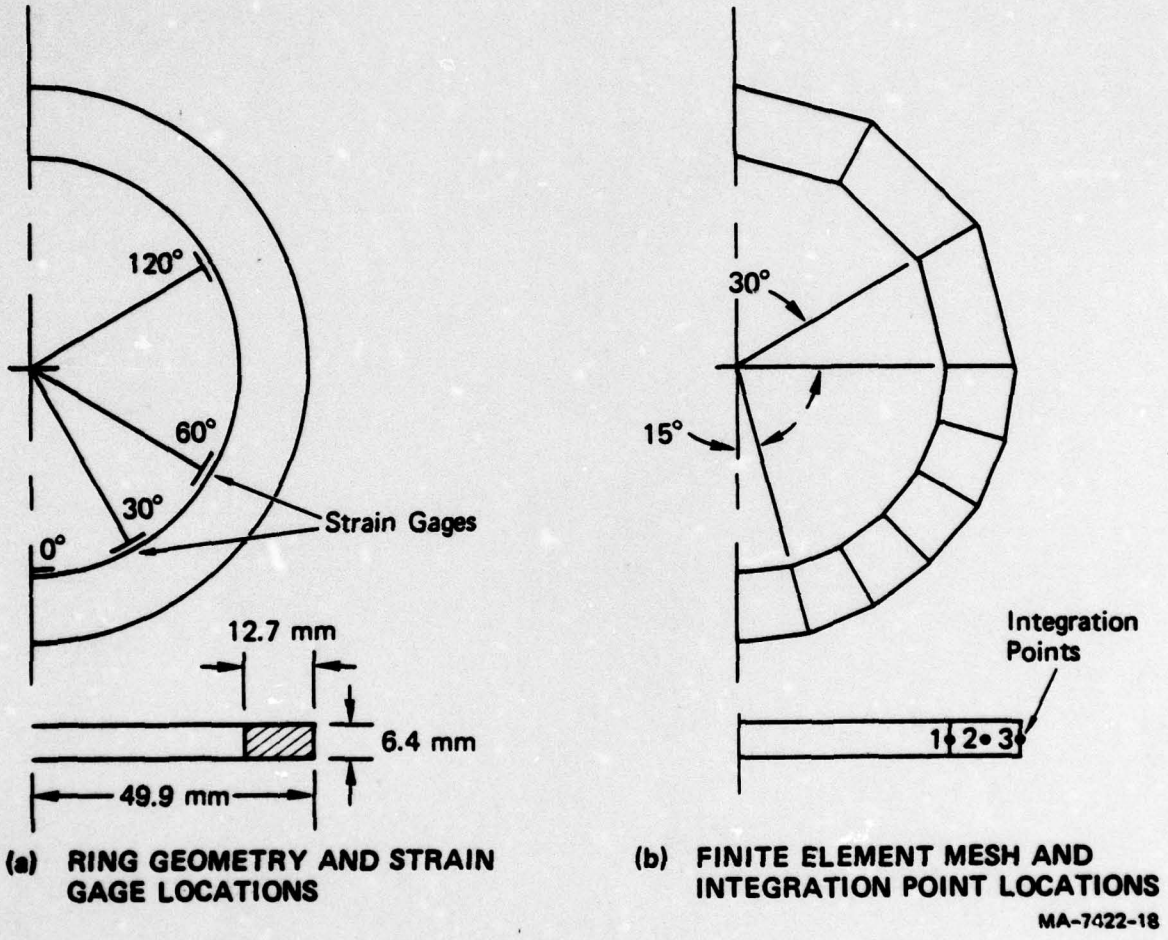

(a) RING GEOMETRY AND STRAIN GAGE LOCATIONS

(b) FINITE ELEMENT MESH AND INTEGRATION POINT LOCATIONS

MA-7422-18

FIGURE 2 FLAT RING GEOMETRY AND FINITE ELEMENT MODEL

Impact point is at 0° position.

The strain records from the flat ring experiment are plotted in Figure 3. The response consists of two phases. The first phase, which lasts for about 200 μs, is the forced response phase during which the ring is in contact with the barrier. The second phase is the free vibration phase, which begins when the ring leaves the barrier. During the initial forced response phase, the deformation is so concentrated near the impact point that the front portion of the ring begins to rebound before the back portion of the ring has stopped. This is seen in the strain records as a decrease in the strain at 0° from about 60 μs to about 110 μs. Subsequently, the momentum of the back portion of the ring forces the front of the ring onto the barrier again, causing a second rise in the strain at 0°. Around 200 μs, the velocity of the entire ring is reversed and the ring leaves the barrier. The strain at 0° falls off, denoting the end of the forced response phase and the beginning of the free vibration phase.

During the free fibration phase, the ring responds in the second, third, and fourth modes of free flexural vibration. The calculated periods[2] of these modes are 243, 85, and 45 μs, respectively. The second mode is the ovalling mode and is most easily seen in the strain record from the 0° location. A sinusoidal waveform with a period of 243 μs is superposed on the record in Figure 3(a). The third mode is the triangular mode and is most easily seen in the strain records from the 60° and 120° locations, since at these locations the amplitude of the second mode is small. A sinusoidal waveform with a period of 85 μs is superposed on the record in Figure 3(c). The fourth mode is discernible in the record from the 30° location, where the amplitude of the second and third modes are small. A sinusoidal waveform with a period of 45 μs is superposed on the record in Figure 3(b).

The finite element model used to analyze this experiment is illustrated in Figure 2(b). The ring model comprises nine beam elements, representing 15° arcs and 30° arcs of the ring. The integration points shown in the figure are used to numerically evaluate the nodal forces and moments. By using a modified trapezoidal integration scheme, it is

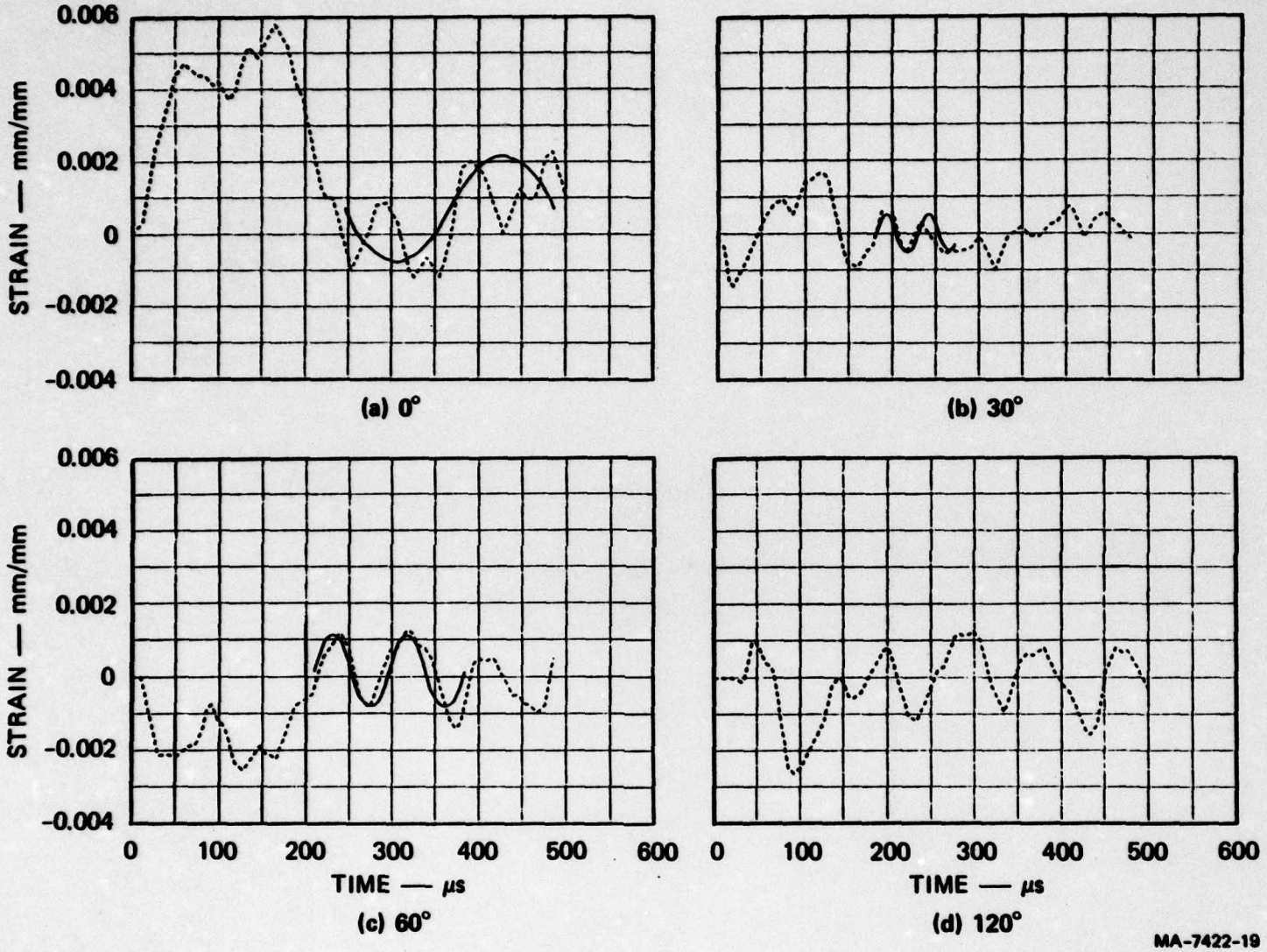

FIGURE 3 STRAIN RECORDS FROM FLAT RING IMPACT AT 6.9 m/s

Impact point is at 0° location.

possible to preserve the exact elastic bending stiffness of the element. The beam cross section is divided into strips, and the axial stress is allowed to vary lineraly across each strip. The total nodal forces and moments are then found by adding the contributions of all the strips. In the calculation, the barrier was modeled as ideally rigid. That is, all the ring nodes were given an initial velocity of 6.9 m/s and the leading node was stopped in a single time step of 1 μs.

A comparison between the calculation and the experiment was made by comparing the strains calculated at integration point 1 [see Figure 2(b)] with the strains measured by the strain gages. This comparison is shown in Figure 4. The general shape and the magnitude of the measured and predicted strain histories are in good agreement. However, the calculated strains include a high-frequency response not seen in the experiment. The high-frequency response corresponds to the highest mode of the finite element model, which is excited by stopping the leading node of the ring in only 1 μs.

To allow a more meaningful comparison, the calculated strain histories were numerically filtered at a cut-off frequency of 40,000 Hz. The comparison given in Figure 5 shows that filtering the calculated response gave good agreement between the experiment and the calculation. We conclude that the finite element model accurately predicts the forced response and the free vibration response, except that it includes a high-order mode of flexural vibration.

It is recognized that postprocessing the calculated ring response is not feasible for calculations involving the interaction of the ring, bolts, and plate. However, it was determined in later calculations that the high frequency ring response is greatly inhibited by the shell in calculations of the complete structure. Thus, filtering the predicted response of the ring alone serves to help develop the ring model, but is not necessary in calculations of a multicomponent structure.

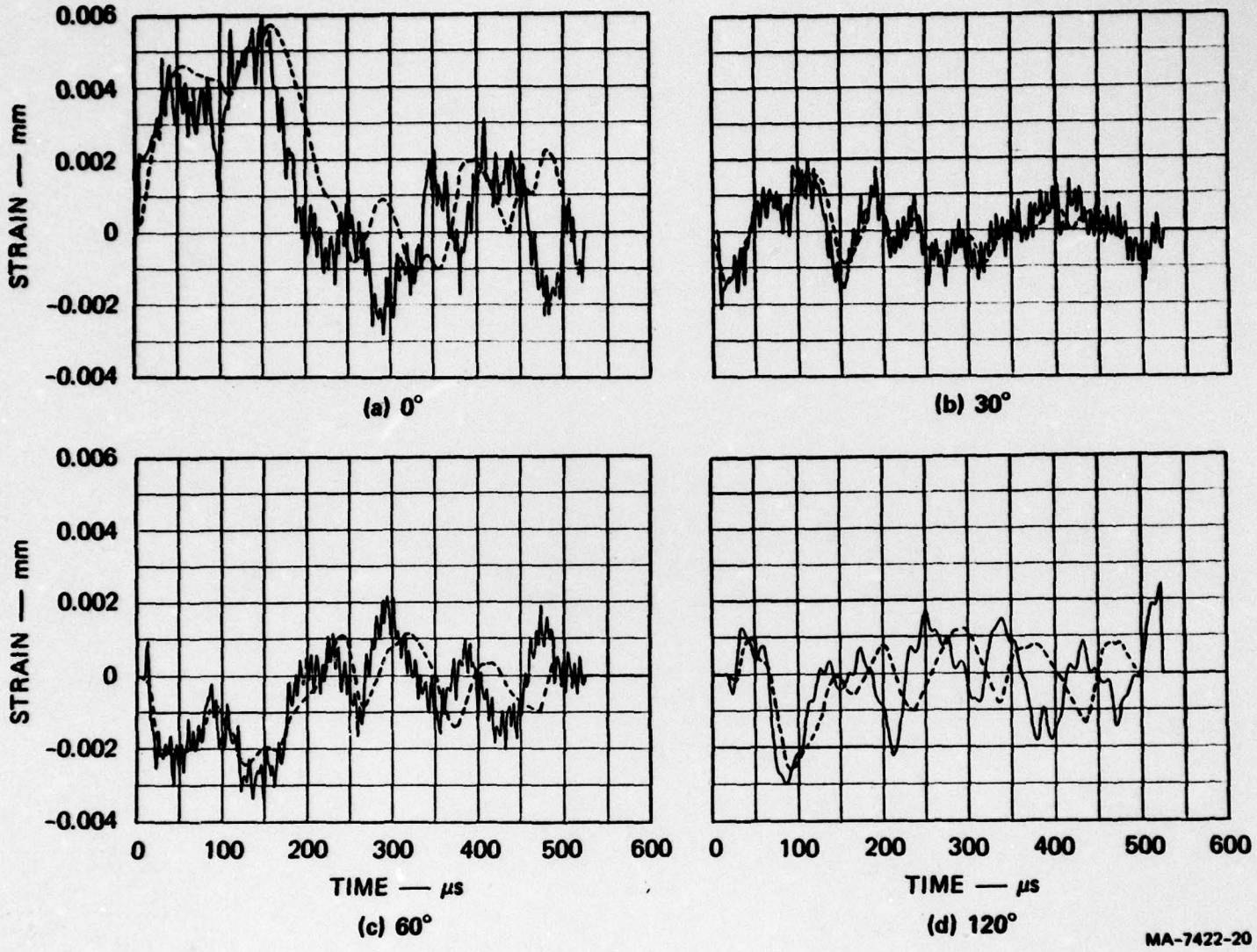

FIGURE 4 COMPARISON OF CALCULATED AND MEASURED STRAINS FROM FLAT RING IMPACT AT 6.9 m/s

Impact point is at 0° location. ------ Experiment ——— Calculation

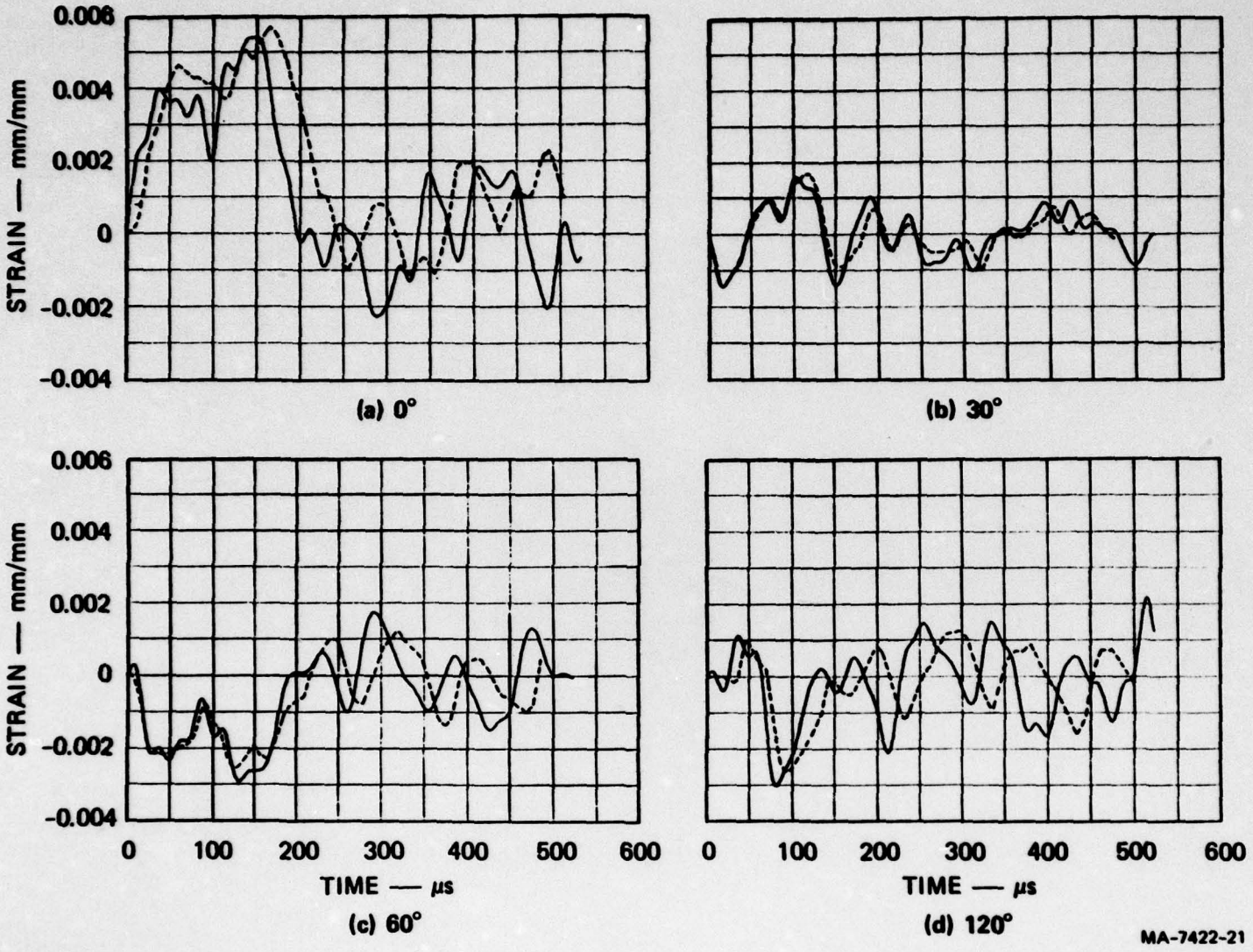

FIGURE 5 COMPARISON OF FILTERED CALCULATION AND MEASURED STRAINS FROM FLAT RING IMPACT AT 6.9 m/s

Impact point is at 0° location. ------ Experiment ——— Calculation

Elastic Response of an L-Section Ring

The second experiment in the ring study was a low-speed impact of an L-section ring without a shell. This experiment was conducted so that a ring with an L-section could be studied without the added complexity of plasticity or shell effects. The web and flange of the ring section measured 10.8 mm by 1.3 mm; the outside diameter was 99.8 mm. The ring geometry is shown in Figure 6(a). The ring material was 6061-T6 aluminum. Circumferential strain gages with an element length of 6.4 mm and a width of 0.5 mm were mounted at several locations on the top of the flange at the inside edge of the ring. The gage locations are also shown in Figure 6(a). The ring was launched so that it struck the steel barrier edge-on in free flight at a speed of 5.2 m/s.

The strain records from this experiment are plotted in Figure 7. As with the flat ring, the L-section ring shows a forced response phase and a free vibration phase. Again, the double peak in the strain at 0° is seen during the forced response phase. The calculated periods of the second, third, and fourth modes of flexural vibration are 225, 80, and 45 μs, respectively.

For the calculation of this experiment, the ring model consisted of nine beam elements with an L-shaped cross section. The mesh and element geometry are shown in Figure 6(b). The strains calculated at integration point 1 were compared with experimental values. The impact was again modeled by stopping the leading node in a single time step. High-frequency vibrations were again predicted in the calculation, and these were filtered as before to allow comparison with experimental values.

The comparison between predicted and measured strain in the elastic L-ring is shown in Figure 8. In general, the agreement is good. The major differences are attributed to possible out-of-plane bending in the experiment, a phenomenon that was not permitted in the calculation. This phenomenon is considered to be unimportant in a ring attached to the shell.

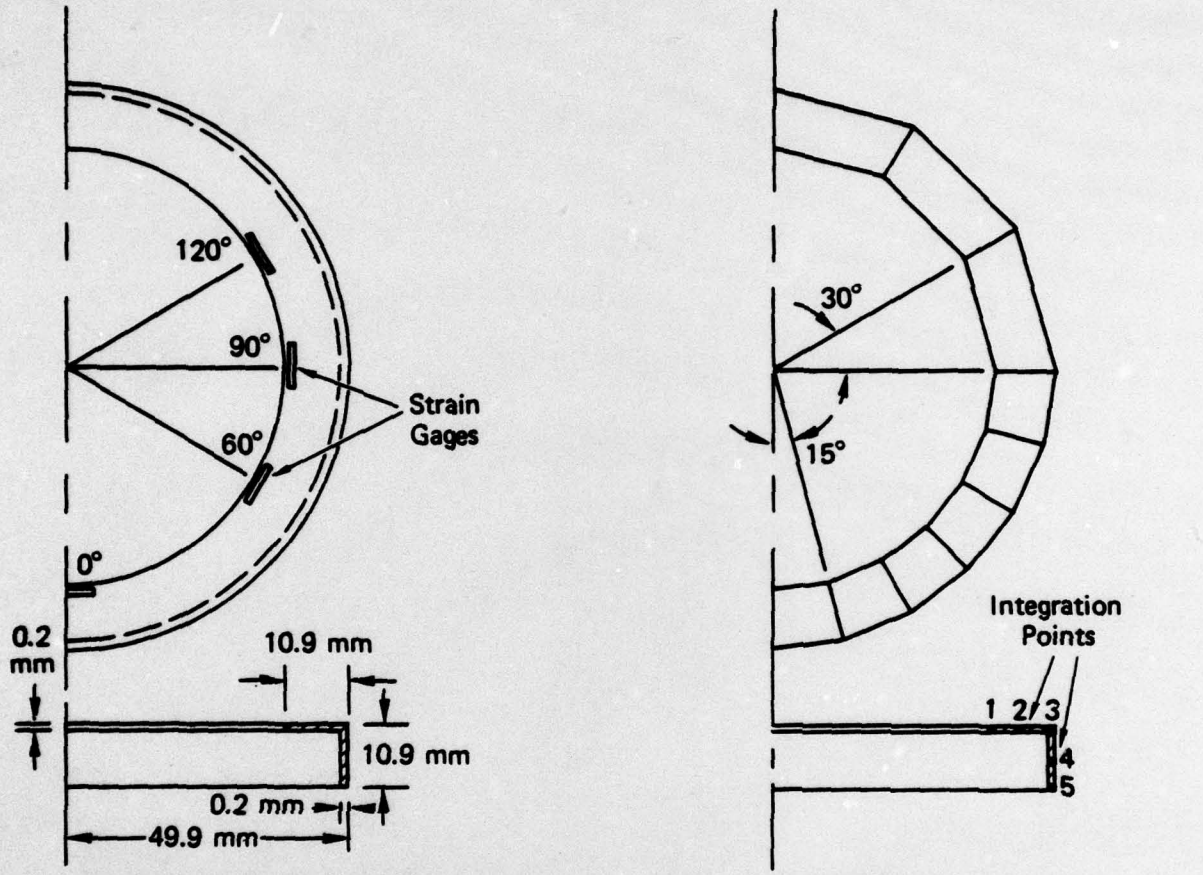

(a) RING GEOMETRY AND STRAIN GAGE LOCATIONS

(b) FINITE ELEMENT MESH AND INTEGRATION POINT LOCATIONS

MA-7422-22

FIGURE 6 L-SECTION RING GEOMETRY AND FINITE ELEMENT MODEL

Impact point is at 0° location.

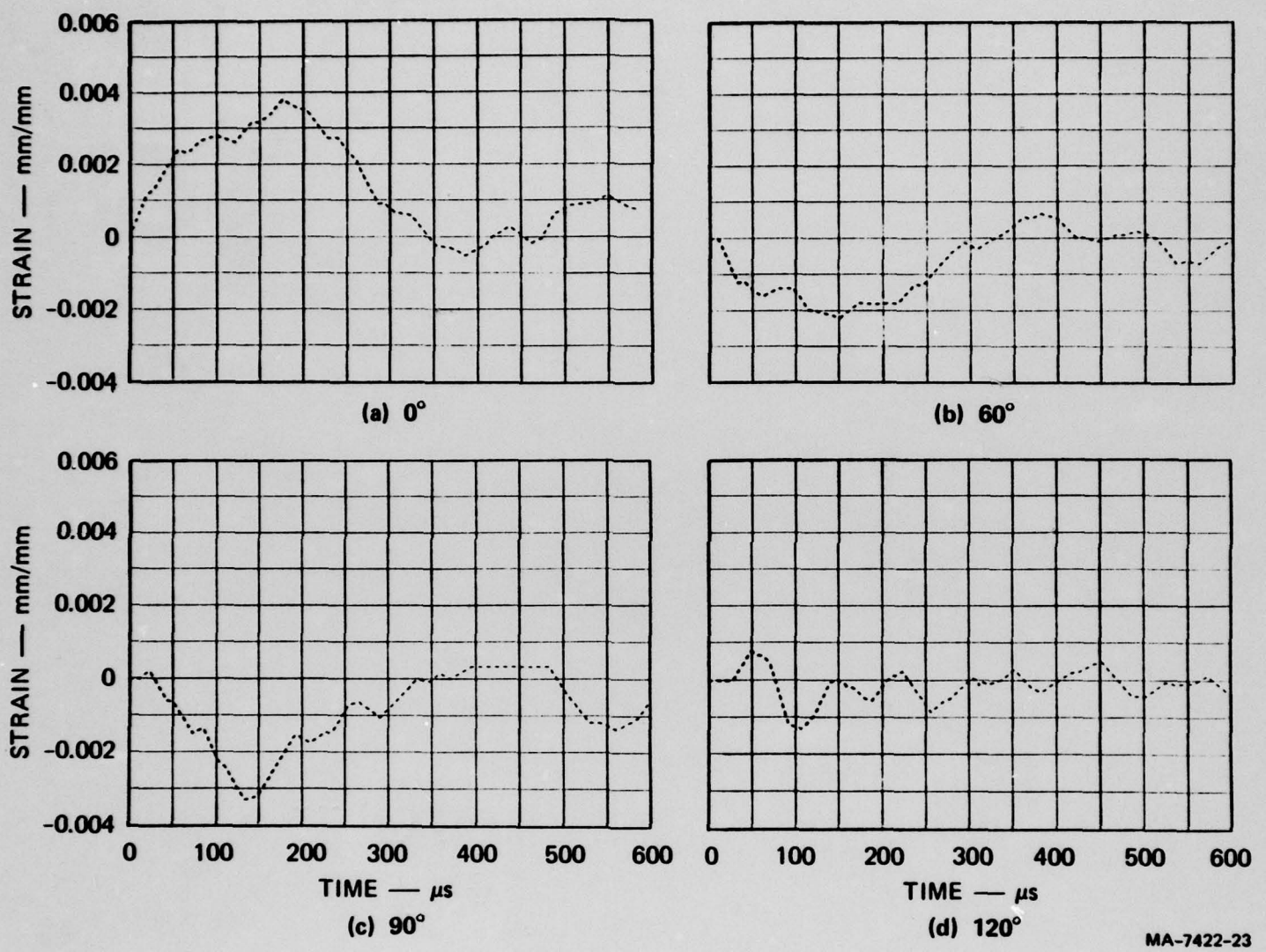

FIGURE 7 STRAIN RECORDS FROM L-RING IMPACT AT 5.2 m/s

Impact point is at 0° location.

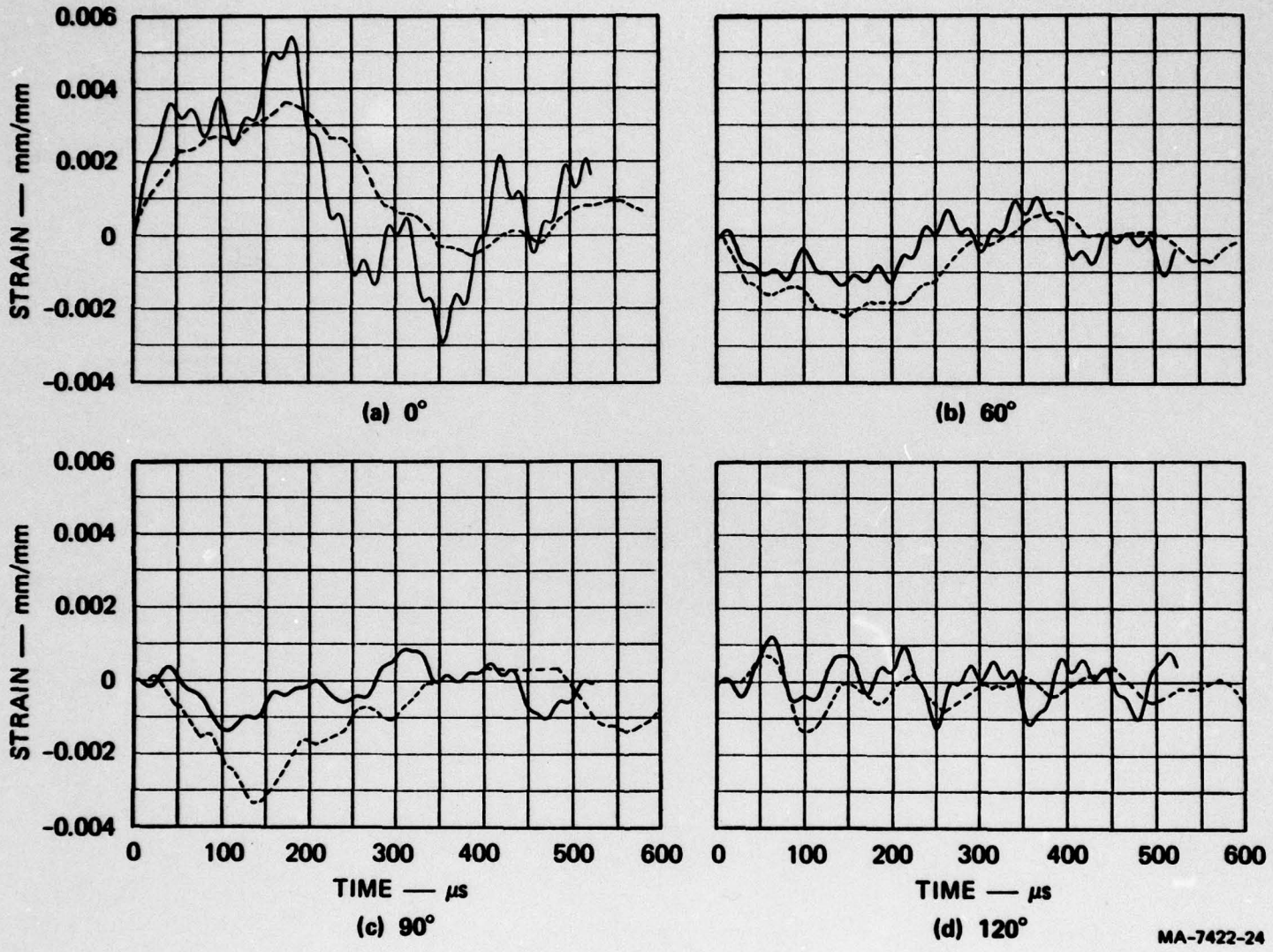

FIGURE 8 COMPARISON OF FILTERED CALCULATION AND MEASURED STRAINS FROM L-RING IMPACT AT 5.2 m/s

Impact point is at 0° location. ------ Experiment ——— Calculation

Elastic-Plastic Response of an L-Section Ring

The third experiment in the ring study was a higher speed impact of an L-section ring without a shell. This experiment was conducted so that the effect of plasticity in the ring could be studied. The ring was launched so that it struck the steel barrier edge-on in free flight at a speed of 10.4 m/s. The ring tested was the same one used in the low-speed impact experiment. Although a slight amount of plastic flow occurred in the low-speed impact test, the ring was essentially undeformed and the properties were essentially unchanged, owing to the small hardening modulus of 6061-T6 aluminum.

The strain records from the third ring experiment are plotted in Figure 9. The forced response phase and the free vibration phase are again apparent. During the forced response phase, a plastic hinge is formed at the impact point at about 50 μs and large strains are recorded at 0°. As in the previous experiments, the concentrated deformation causes the front of the ring to rebound. However, the momentum of the back end of the ring forces the front end of the ring into the barrier, causing a second rise in the strain at 0°. A precursor of this event is seen in the train record at 90° where another plastic hinge forms at about 130 μs, just before the second rise in the strain at 0°. (The yield strain is about 0.004 mm/mm.)

In the calculation of this experiment, we used the same element mesh used for the low-speed impact [see Figure 6(b)]. A yield stress of 307 MPa and a hardening modulus of 724 MPa were used for the 6061-T6 aluminum. Again, high frequency vibration response was filtered out of the predicted strain records for comparison with experimental values.

The experiment and calculation are compared in Figure 10. Qualitatively, the agreement is good. The strain magnitudes at 0° are also predicted very well during the 150 μs of the response.

L-Section Ring in a Shell

In the last experiment in the ring study, an L-section ring was riveted into a shell and launched into the barrier to study the effect

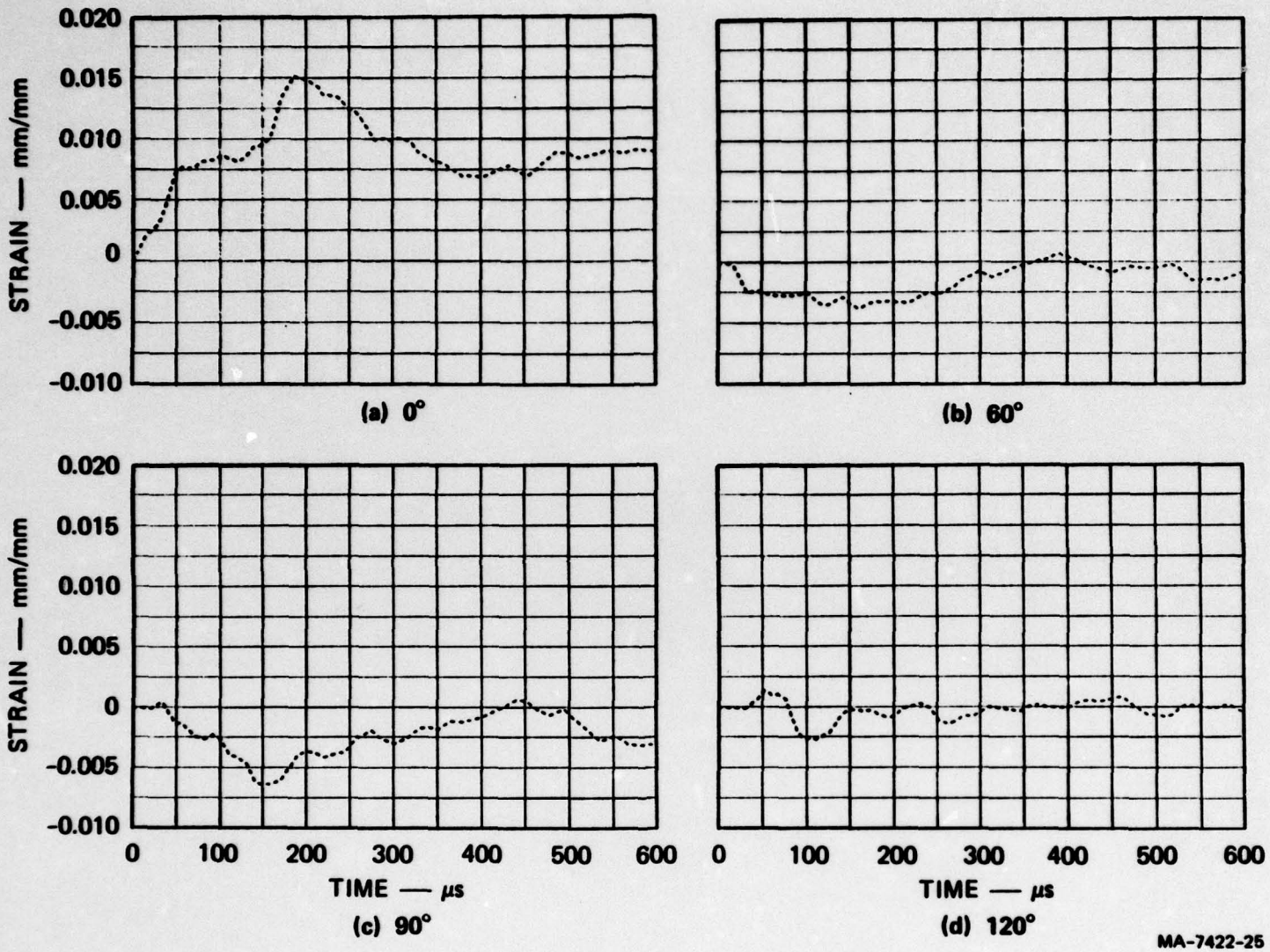

FIGURE 9 STRAIN RECORDS FROM L-RING IMPACT AT 10.4 m/s

Impact point is at 0° location.

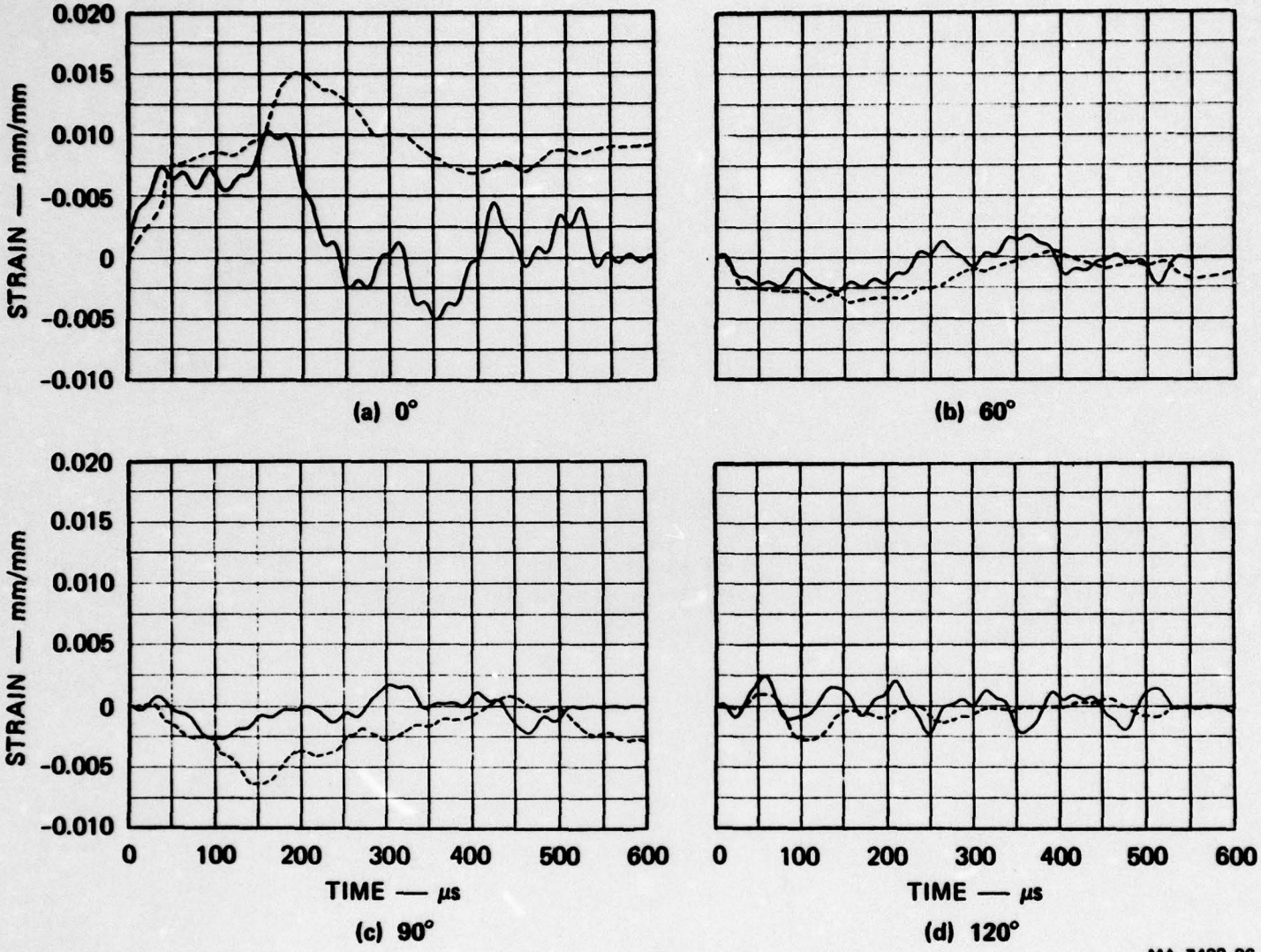

FIGURE 10 COMPARISON OF FILTERED CALCULATION AND MEASURED STRAINS FROM L-RING IMPACT AT 10.4 m/s

Impact point is at 0° location. ------ Experiment ——— Calculation

of the shell. The geometry of the ring and shell are shown in Figure 11(a). Strain gages were located at 0°, 60°, 90°, and 120°. The assembly was launched into the barrier at a free-flight velocity of 5.2 m/s.

The strain records from the experiment are shown in Figure 12. The effect of the shell is to greatly increase the strains and also increase the rise time of the response (compare Figure 7 with Figure 12). This suggests that the shell adds more inertia than strength.

To calculate the response observed in this experiment, the ring model was modified by adding mass to the nodes of the beam elements, as illustrated in Figure 11(b). The mass represents the portion of the shell that is stopped by the ring. This is assumed to be a 102-mm length, since the 51 mm of shell below the L-ring is unsupported and the 102 mm above the ring is shared with the end ring.

A comparison of the experiment and the unfiltered calculation is shown in Figure 13. In this case, the shell greatly inhibits the high frequency response of the ring in the calculation so that filtering is unnecessary. Qualitatively, the agreement between the calculation and the experiment is good; however, the predicted magnitude of the strains is too low. This may be due to the fact that the shell mass was added at the centroid of the ring section rather than at the center of the shell wall. It is estimated that this effect could increase the strain at 0° by about 20%. Unfortunately, the mass can only be added at the centroids of the ring elements.

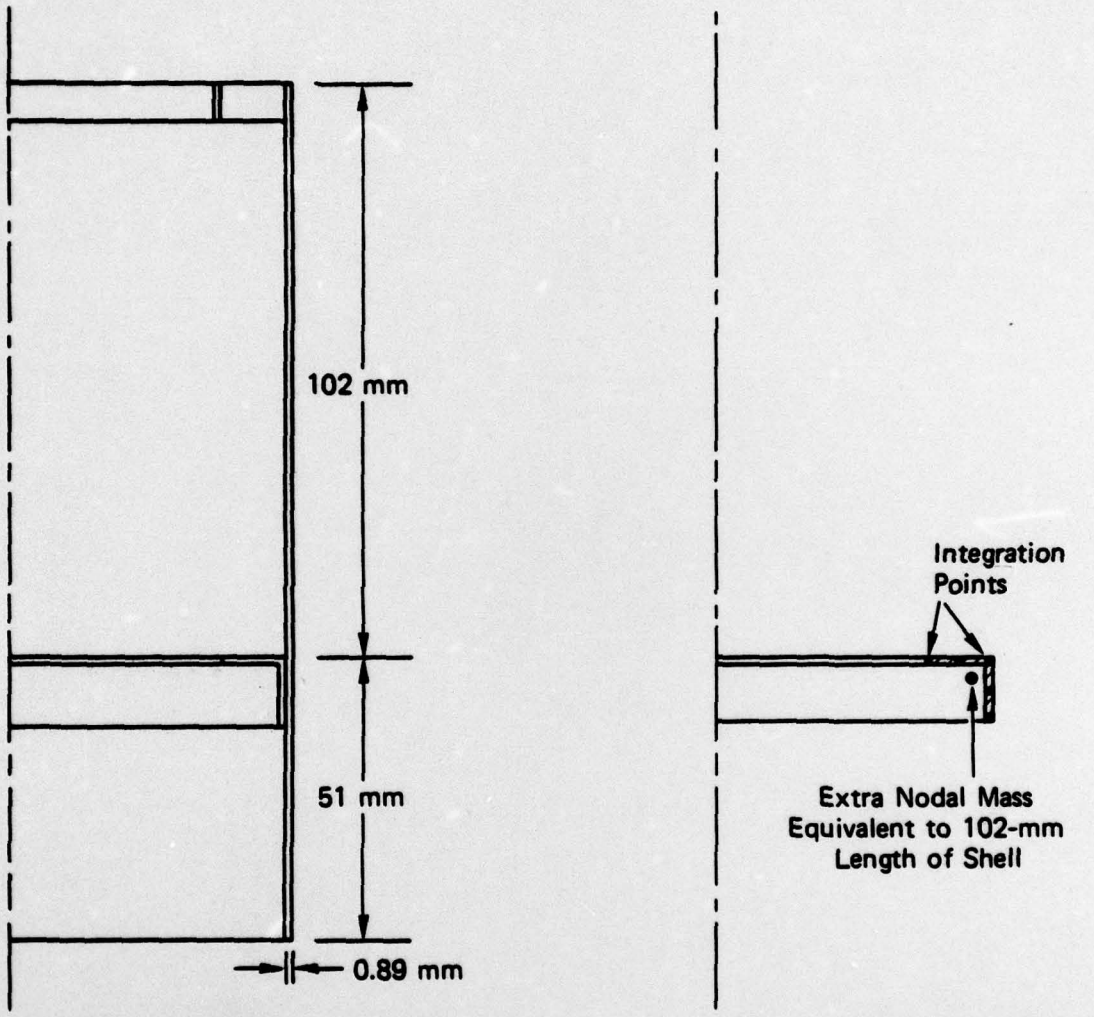

FIGURE 11 L-SECTION RING AND SHELL GEOMETRY AND FINITE ELEMENT MODEL

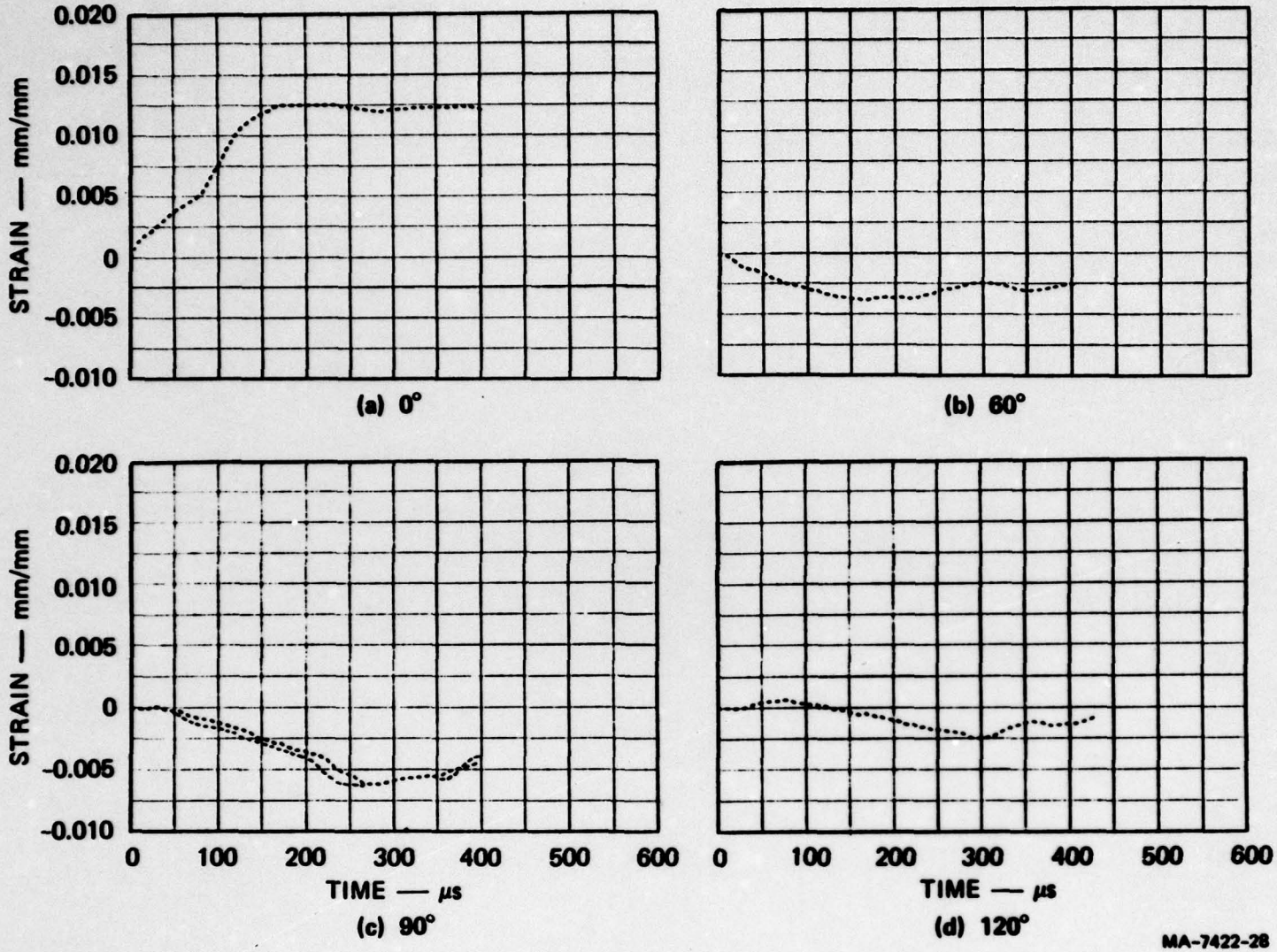

FIGURE 12 STRAIN RECORDS FROM L-RING AND SHELL IMPACT AT 5.2 m/s

Impact point is at 0° location.

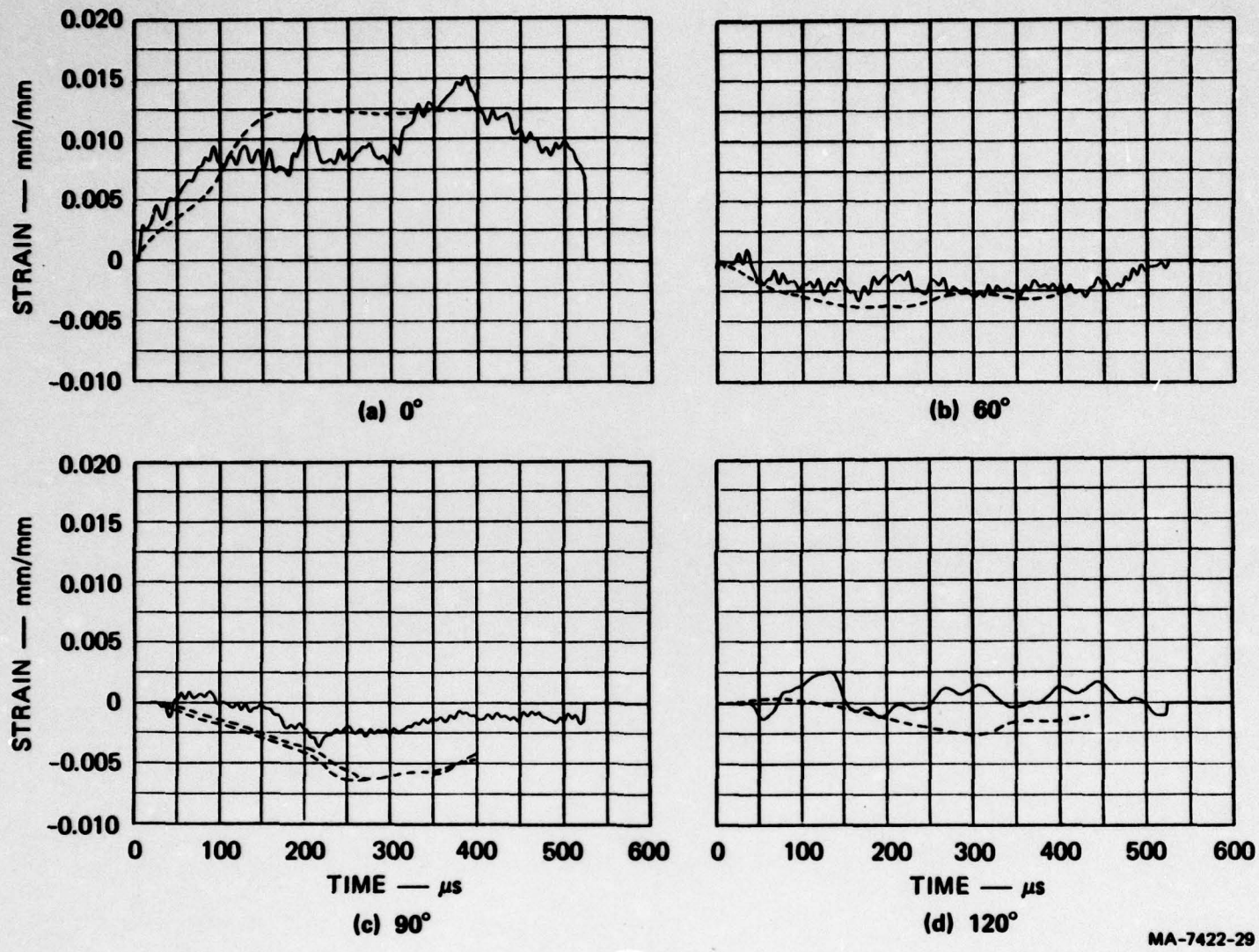

FIGURE 13 COMPARISON OF UNFILTERED CALCULATION AND MEASURED STRAINS FROM L-RING AND SHELL IMPACT AT 5.2 m/s

Impact point is at 0° location. ------ Experiment ——— Calculation

III FINANCIAL STATUS

As of September 1979, $68,042 has been spent on labor (1359 supervisory and professional hours, 811 technical and clerical hours), and $3678 has been spent on materials and services. Of the total contract funds ($93,441), the balance remaining is $16,720. A performance and cost report for this period is attached.

PERFORMANCE AND COST REPORT
DAAK-10-78-C-0158
PYU-7422 - Report No. 8

Reporting Period: 3 July - 2 September 1979

Hours

Total hours expended to date:

Supervisory and Sr. Professional Personnel	270
Professional Personnel	1089
Technician	811
Cumulative total hours to date	2170
Percent of total hours expended to date	95%

Funds

Funds expended during the reporting period	$ 5,047
Funds expended to date	76,720
Percent of total funds expended to date	85%

Work

Percent of work completed during the reporting period	10%
Percent of work completed to date	90%

REFERENCES

1. J. D. Colton, J. K. Gran, and H. E. Lindberg, "Response of Adaption Kits in Side Impacts," Interim Report for the Department of the Army, Contract DAAA21-76-C-0076 (February 1978).

2. W. Flugge, ed., *Handbook of Engineering Mechanics*, (McGraw Hill, New York, 1962).